

Proc. NIPR Symp. Upper Atmos. Phys., 7, 40–52, 1994

## CONSIDERATION OF DYNAMIC SPECTRA AND DIRECTION FINDING RESULTS OF HISS-TRIGGERED CHORUS EMISSIONS

Katsumi HATTORI<sup>1</sup> and Masashi HAYAKAWA<sup>2</sup>

<sup>1</sup>*Department of Electronics and Informatics, Faculty of Engineering,  
Toyama Kenritsu University, Kosugi, Toyama 939-03*

<sup>2</sup>*Department of Electronics Engineering, The University of Electro-Communications,  
5-1, Chofugaoka 1-chome, Chofu-shi, Tokyo 182*

**Abstract:** Based on our previous experimental results of hiss-triggered chorus emissions and the theory of Helliwell, we propose a possible mechanism for how a chorus emission is generated from a wavelet in the hiss band. It consists of two steps: the phase bunching process of the resonant electrons and the radiation process. We select a VLF event observed onboard satellite GEOS1 on July 21, 1977 and verify the proposed mechanism computationally. Whether the phase bunching occurs or not is examined to investigate the phase bunching time, the resonance time, and the duration of the wavelet. The validity of the generation model is considered through the reconstruction of chorus elements with use of three-dimensional ray tracing computations. Special attention is paid to the slope of the chorus elements and the frequency dependence of the wave normal angles for a chorus element. The theoretically reconstructed chorus element which satisfies the temporal variations onboard the satellite is found to occur with the Gendrin angle for the generation angle at the equator. Furthermore, there is a tendency for the generation angle to the Earth's magnetic field to shift to a larger angle with increase of frequency and to terminate around the oblique resonance angle. Propagation after the radiation is also found to be in the non-ducted mode through the computations.

### 1. Introduction

Magnetospheric VLF/ELF emissions are classified into two different types: (1) unstructured hiss and (2) structured and discrete chorus (*e.g.*, HELLIWELL, 1965; SAZHIN, 1982; HAYAKAWA *et al.*, 1990; SAZHIN and HAYAKAWA, 1992). However, fundamental problems, including whether these two types of emissions are essentially different or not and the link between the two, are still unsolved, and further investigation is required. In order to clarify these problems, studying the hiss-triggered chorus events is of great importance.

The generation mechanism of spontaneous chorus emissions has been studied experimentally by BURTON and HOLZER (1974), GOLDSTEIN and TSURUTANI (1984), and HAYAKAWA *et al.* (1984), and theoretically by NUNN (1974), BESPALOV and TRAKHTENGERTS (1974), and CURTIS (1978). Being closely associated with the generation of spontaneous chorus, there have been proposed two possibilities as the stimulus to trigger a chorus, which seem to contradict each other. The first one is hiss which has so far been considered to be very random and turbulent, because the

ground and satellite VLF/ELF measurements have indicated that chorus is frequently accompanied by a background of hiss (BURTIS and HELLIWELL, 1976; CORNILLEAU-WEHRLIN, 1978; KOONS, 1981). The second candidate is power line harmonic radiation (PLHR) (LUETTE *et al.*, 1977, 1979) which is monochromatic and coherent in nature. By using the events of hiss-triggering chorus observed on the SCATHA satellite, KOONS has arrived at the conclusion that some structures or large-amplitude spectral components existing in the hiss band are able to phase-bunch the electrons, leading to the excitation of chorus emissions (KOONS, 1981). But the experimental data reported by KOONS are not persuasive that hiss is a source of chorus. Therefore, more extensive experimental studies are required. For this aim, we have performed detailed signal analyses (HATTORI *et al.*, 1991a, b).

The following important results are obtained: (1) Each chorus element has a tendency to originate from the hiss band and is asymptotic to the hiss band. (2) The intensity and occurrence of chorus are closely correlated with the intensity of the underlying hiss. (3) The hiss has been so far considered to be random and incoherent, but it exhibits some structures or wavelets, which are monochromatic wave components with significant duration, and we notice the existence of the causative wavelet at the foot of each chorus element. (4) When we expect a chorus to be triggered from a wavelet at the upper edge of the hiss band, the duration of the wavelet increases with decreasing intensity. (5) Very similar  $\phi$  values of the azimuth are noticed for both hiss and chorus, suggesting that both phenomena come from the same source region. These experimental results suggest that hiss has an important role in the generation of chorus in the outer magnetosphere. Furthermore, these facts lead us to conclude that a wavelet existing at the upper edge of the hiss band is able to generate a chorus emission through the coherent wave-particle interaction in the outer magnetosphere, as in the case of active VLF wave injection experiments.

In the present paper, a generation mechanism of hiss-triggered chorus emissions is proposed based on the experimental results, and its validity is investigated paying attention to the temporal changes of dynamic spectra such as the chorus slope and the frequency dependence of the wave normal angle observed onboard the satellite.

## 2. Summary of the Experimental Findings

The results of detailed spectral analyses and direction finding for both VLF and ELF data containing simultaneous hiss and chorus have been reported on the basis of the data observed onboard the GEOS1 satellite (HATTORI *et al.*, 1991a, b). Table 1 shows the analyzed data, and the summary is described with some figures in this Section.

Table 1. Analyzed events.

Event	Date	Time (UT)	<i>L</i> value	Geomag. lat (deg)
VLF	1977.7.21	1212:45 – 1241:11	6.5 – 6.8	6.8 – 8.5
ELF	1977.11.19	0548:05 – 0626:43	8.2	22.7 – 23.9
Hiss	1977.6.20	1700:23	6.2	19.7

### 2.1. Characteristics of the dynamic spectra and relationship between hiss and chorus in intensity

A typical spectrogram of hiss-triggered chorus is indicated in Fig. 1. This figure shows the magnetic field component  $b_x$ . The signal below about 900 Hz is called hiss, which seems to be band-limited white noise. Chorus emissions are those which indicate discrete rising-tone structures. It is likely that each chorus element in this figure originates from the upper edge of the underlying hiss band and also that every riser is asymptotic to the hiss band at the beginning, that is, every chorus has a very small initial  $df/dt$  value. The duration of each chorus element is about 1 s and the average  $df/dt$  is about 0.7 kHz/s. Also, the chorus occurrence rate found to be closely correlated to the underlying hiss intensity, that is, the chorus generation, is enhanced when the hiss activity becomes high. The correlation coefficient between hiss (735 Hz) and chorus (1010 Hz) intensity is found to be 0.7. The chorus intensity is about 6 dB higher than the hiss intensity.



Fig. 1. Hiss-triggered chorus event in the VLF range.

### 2.2. Fine structure analyses and wavelets

According to the fine structure analysis with a frequency resolution of 23 Hz and with a temporal resolution of 43 ms, we recognize that some parts of hiss exhibit some island structures or wavelets, which are monochromatic wave components with some duration. We examine the same fine structure analysis of the event which indicates hiss without chorus, and we have some wavelets in the hiss band. This is an important new finding; hiss has so far been considered to be incoherent and turbulent. Furthermore, we can identify a wavelet at the foot of a chorus element, which can be considered to cause the relevant chorus emission.

Figure 2 shows the relationship of the magnetic intensity of wavelets in the hiss band and their duration. A white dot corresponds to a wavelet without chorus; a dark dot represents a wavelet accompanied by chorus in the hiss band. The dots marked ELF (only dark dots) show wavelets from the ELF event; others are from the VLF event. The duration of wavelets for the VLF event ranges from 50 to 150 ms, with an average of about 70 ms. On the other hand, those from the ELF event are considerably longer than those from the VLF event. The best fit to all the dark dots which triggered a chorus is a hyperbola, which provides us with the experimental threshold for exciting a chorus from a wavelet in the hiss band. Another important fact is that the wavelet which contributed to the chorus generation exists at the upper edge of hiss band. Though some wavelets without chorus exceed this threshold, it is confirmed that they are not near the top of the hiss band, but within the hiss band.

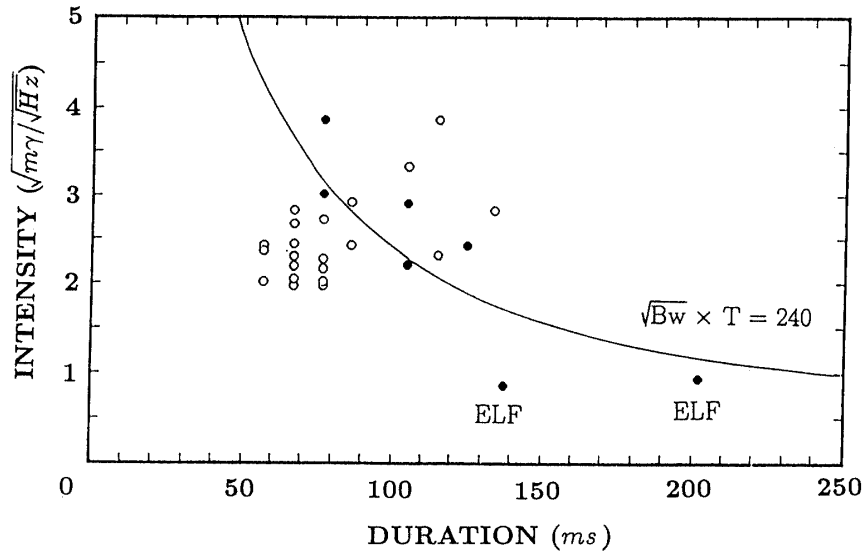


Fig. 2. The relationship between magnetic intensity ( $\sqrt{B_w}$ ) of wavelets and their duration.

### 2.3. Direction finding

The coordinate system for direction finding is defined by the wave normal angle  $\theta$ , which corresponds to the angle between the wave normal direction and the Earth's magnetic field; the azimuthal angle  $\phi$ . The determination of wave normal direction is based on Means' method assuming a single plane wave (MEANS, 1972) with frequency resolution of 23 Hz and time resolution of 43 ms, respectively. The most important direction finding fact is that the same azimuthal values are obtained for

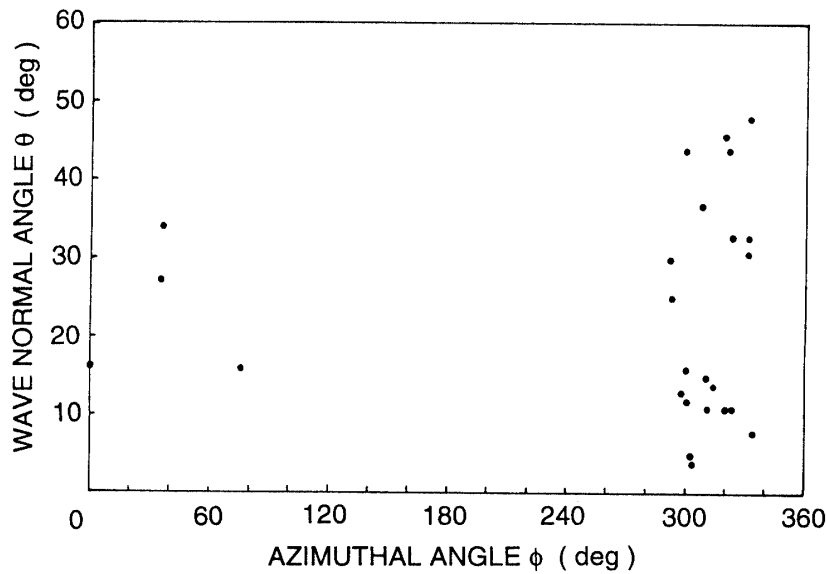


Fig. 3. Direction finding results for VLF events based on the wave distribution method. The vertical and the horizontal axes correspond the wave normal angle  $\theta$  and the azimuthal angle  $\phi$ .

hiss and chorus, which implies that both hiss and chorus come from the same source region. Figure 3 illustrates direction finding results for chorus based on the wave distribution function method using the maximum entropy method (STOREY and LEFEUVRE, 1979). The horizontal and vertical axes correspond to the wave frequency and the wave normal angle  $\theta$ . The direction finding results are consistent with those of the Means method.

### 3. Generation Mechanism of the Hiss-Triggered Chorus

It is found that there are many structures or wavelets within the hiss band by performing fine structure analysis. This seems to hold a universally for the hiss, though hiss has so far been considered to be incoherent and turbulent. Moreover, as for the analyzed events, it is found that a chorus element is likely to have originated from a causative wavelet just at the foot of the chorus element. Also, a chorus element is asymptotic to the hiss band. The direction finding results of both VLF and ELF hiss-triggered chorus emission show that the azimuthal angle  $\phi$  values for both hiss and chorus are the same, suggesting that both phenomena come from the same source region. These experimental results lead us to the conclusion that a chorus is triggered from a wavelet existing at the upper edge of the hiss band through a coherent wave-particle interaction in the case of an active VLF injection experiment (HELLIWELL *et al.*, 1986).

Based on the experimental results and Helliwell's theory (HELLIWELL, 1967), the following generation model for hiss-triggered chorus emission is considered. At first, the energetic resonant electrons, with a wavelet which has enough intensity and duration and is located at the upper edge of the pre-existing hiss band, are phase-bunched at the magnetic equator in the outer magnetosphere. Then, these phase-bunched electrons move away from the equator along the earth's magnetic field line, radiating a coherent wave which satisfies the cyclotron resonance condition and the dispersion condition at any latitude  $\Lambda$ ; this causes a temporal change of frequency. The radiated wave propagates toward the equator and is detected at the satellite. The generation model is illustrated in Fig. 4.

#### 3.1. Phase bunching

As for the VLF event, the parameters at the equator are obtained from the observed satellite data, using the magnetic dipole model and the diffusive equilibrium model. The equatorial gyrofrequency  $f_{\text{Heq}}$  and the equatorial plasma frequency  $f_{\text{Peq}}$  are 2.853 kHz and 19.7 kHz, respectively. Assuming that the frequency of the causative wavelet in the hiss band is 0.9 kHz, we find that the longitudinal energy is about 5.5 keV, which means the parallel component of the resonant electrons along the earth's magnetic field line. We assume the pitch angle of the resonant electrons to be  $\alpha_{\text{eq}} = 45^\circ$ , and the total energy is found to be about 11 keV. Taking into account the change of plasma parameters along the field line, the emission frequency is obtained from the cyclotron resonance condition and the dispersion equation.

$$\omega - \vec{k} \cdot \vec{v} = \omega_{\text{H}}, \quad (1)$$

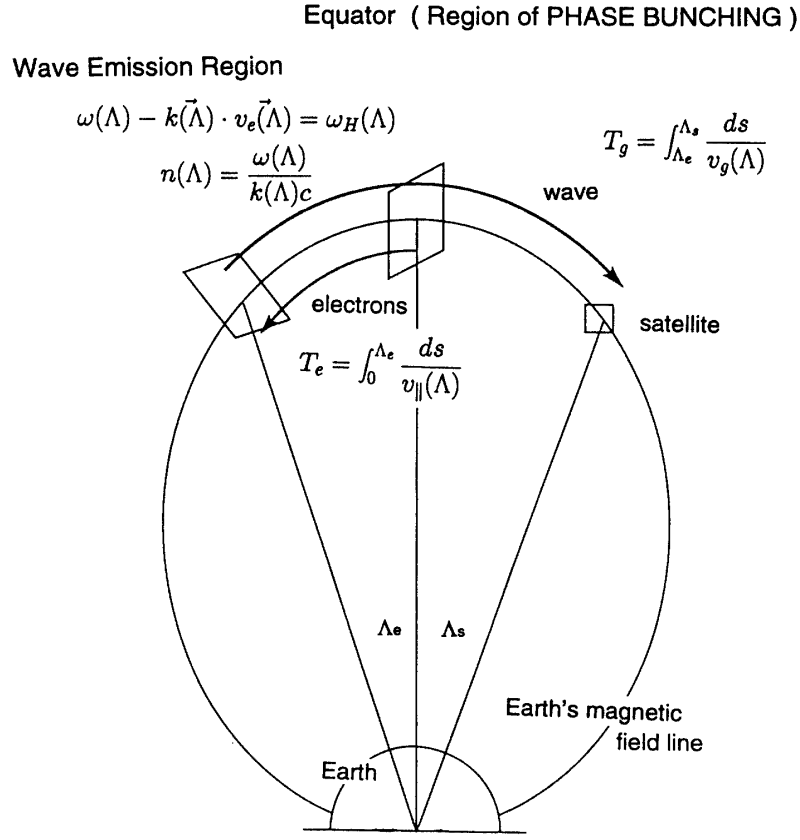


Fig. 4. The generation model of the analyzed chorus emissions.

$$n = kc / \omega , \quad (2)$$

$\omega$ ,  $\omega_H$ ,  $k$ , and  $v$  are wave frequency, gyrofrequency, wave number, and resonant velocity of electrons, respectively.  $n$  and  $c$  denote the refractive index and velocity of light. Let us assume simple generation, that is, the waves are generated through cyclotron resonance with the generation angle  $\theta_0 = 0^\circ$  at an arbitrary latitude. The required longitudinal energy of resonant electrons decreases with latitude, and the ideal emitted frequency obtained from above equations depends on the generation latitude as shown in Fig. 5. The uppermost frequency of chorus is about 1.6 kHz as shown in Fig. 1. Therefore, the radiation region is considered to extend up to about  $15^\circ$  latitude. Here, we investigate the possibility of the phase bunching of resonant electrons by the wavelet at the upper edge of the hiss band through the phase bunching time  $T_b$  (HELLIWELL, 1967) and the wave-particle interaction time  $T_r$  (HELLIWELL, 1967; SCHULZ, 1972).  $T_b$  is defined by the following

$$T_b = \frac{\pi}{8} \sqrt{\frac{m}{e} \frac{\lambda}{v_{\perp} B_w}} , \quad (3)$$

$m$ ,  $e$ ,  $v_{\perp}$ ,  $\lambda$ , and  $B_w$  denote electron mass, electron charge, transverse velocity of the resonant electron, wavelength of the wavelet, and magnetic intensity of the wavelet,

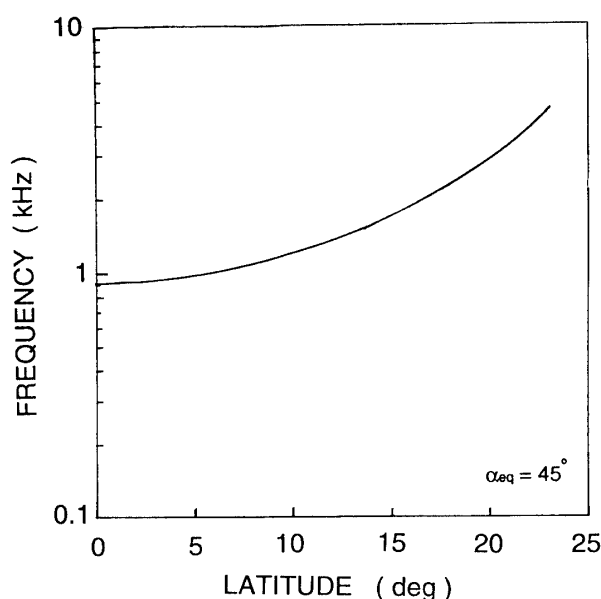


Fig. 5. The latitudinal change of the radiation frequency.

respectively. The intensity of the wavelet with relevant chorus is found to be about  $10 \text{ m}\gamma/\sqrt{\text{Hz}}$  from Fig. 2. Assuming the wavelet band width in the hiss band to be 4 Hz, the magnetic intensity is about  $20 \text{ m}\gamma$ ; then  $T_b$  is about 10 ms. There are two ways to obtain  $T_r$ : one is a method using the interaction region (HELLIWELL, 1967), and the other, with use of the intrinsic band width (SCHULZ, 1972).  $T_r$  is found to be about 100 ms from both calculations. Then, it is found that  $T_b < T_D \sim T_r$ .  $T_D$  means the duration of the causative wavelet. This indicates that the wavelet has a capacity to phase bunch the resonant electrons.

There are many papers dealing with the nonlinear interaction between resonant electrons and a monochromatic whistler-mode wave. Test particle simulation of phase bunching of two waves whose frequencies are slightly different from each other has been reported (MATSUMOTO and OMURA, 1981). When the frequency difference is greater than twice the trapping frequency  $\omega_t$ , electrons which are trapped by the first wave are not detrapped by the second wave, assuming that both waves have the same amplitude. As for the VLF event,  $2\omega_t$  becomes about 30 Hz based on the satellite observation. Therefore, the wavelet at the upper edge of the hiss band is considered to have a capacity to phase-bunch the resonant electrons at the magnetic equator; these phase-bunched electrons are not detrapped by another wavelet whose frequency is separated by more than 30 Hz. On the other hand, SA (1990) reports that triggered emissions can occur even if the amplitude ratio of two waves is very small, on the basis of a test particle simulation. That is, a wave can be perturbed by much weaker signals within  $2\omega_t$  of itself, and the weaker wave plays an important role in triggering new waves. Further research is required to explain the micro-process of hiss-triggering chorus emissions.

### 3.2. Dynamic spectra

The reconstruction of dynamic spectra is considered in this Section. The relevant chorus is radiated through the cyclotron instability with two steps mentioned above. The dynamic spectrum is reproduced in the following procedure. The emitted frequency changes with latitude as shown in Fig. 4, and the time which is required for the whole emission process is given by the sum of electron traveling time  $T_e$  from the equator to the radiation latitude  $\Lambda_e$  and propagation time  $T_g$  of the radiated wave from the radiation point  $\Lambda_e$  to the satellite location  $\Lambda_s$ . With use of the longitudinal velocity of the resonant electrons  $v_{\parallel}$  and the group velocity of the radiated wave  $v_g$ ,

$$T_e = \int_0^{\Lambda_e} \frac{ds}{v_{\parallel}(\Lambda)} , \quad (4)$$

$$T_g = \int_{\Lambda_e}^{\Lambda_s} \frac{ds}{v_g(\Lambda)} . \quad (5)$$

These relationships give us the time dependence of the radiated wave. We obtain  $T_e$  based on the assumption that the electrons move along the field line.  $T_g$  is calculated with use of the three dimensional ray tracing computation. The dipole model and the diffusive equilibrium model are adopted, and the parameter is selected to satisfy the data observed onboard satellite. The satellite location is about  $7^\circ$  in magnetic latitude, about  $18^\circ$  in magnetic longitude, and about 6.7 in  $L$  value. The relationship between the radiated frequency and the latitude is obtained from Fig. 5.

Figure 6 indicates an example of the reconstructed dynamic spectrum.  $T_e$  shows the traveling time of the resonant electrons from the equator to the emission

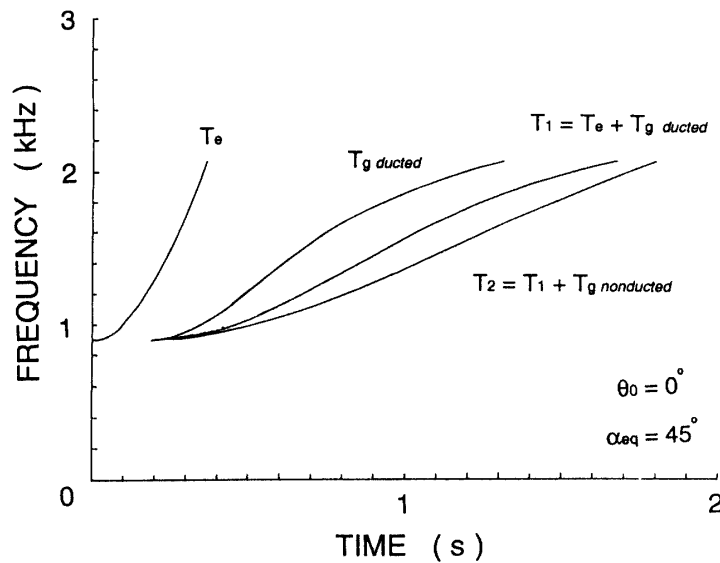


Fig. 6. An example of the reconstructed dynamic spectrum. The generation angle  $\theta_0$  is assumed to be along the magnetic field lines. The results corresponding to ducted and non-ducted propagation are presented.



latitude.  $T_g$  corresponds to the propagation time for ducted propagation, and  $T_1$  is the expected spectrum observed onboard satellite for ducted propagation.  $T_2$  is the theoretical spectrum observed onboard satellite for non-ducted propagation after generation with wave normal angle  $\theta_0 = 0^\circ$ . The average  $df/dt$  is about 1.1 kHz/s and 0.9 kHz/s for ducted and non-ducted propagation, respectively. Since the observed  $df/dt$ , which is linearly fitted, is about 0.7 kHz/s, the reconstruction is not good. Also, the obtained theoretical  $\theta$  values are larger than about  $35^\circ$ . These are different from the observation in Fig. 3.

We note the direction finding results, especially the frequency dependence of the wave normal angle  $\theta$ . We have performed three-dimensional inverse ray tracing based on the direction finding results (Fig. 7). Since the propagation paths are not so far away from the field line within  $15^\circ$  in latitude, the radiation latitude can be estimated from its frequency in Fig. 5. The generation angle  $\theta$ , the Gendrin angle  $\theta_g$  (HELLIWELL, 1965) and the oblique resonance angle  $\theta_{res}$  (HELLIWELL, 1965) are plotted as dark dots, +, and  $\times$ , respectively. There is a tendency that when the chorus frequency is near 0.9 kHz, the generation angle is around the Gendrin angle and at the higher frequency, it shifts toward the oblique resonance angle.

The frequency dependence of  $\theta$  for chorus observed onboard the satellite is indicated in Fig. 8. Each symbol corresponds to one chorus element. This direction finding result is based on Means' method. The ideal wave normal angle  $\theta$  values onboard the satellite for three different generation angles are also described in Fig. 7. The value beside each curve means the generation angle  $\theta_0$  at the source point. These curves are obtained through ray tracing computations based on the presented chorus generation model. The Landau damping is not considered in ray tracing computations though it is not negligible for propagation with large  $\theta$  values such as at the oblique resonance angle  $\theta_{res}$ . Most of the dots exist between the curves labeled  $\theta_g$  and  $\theta_{res} - 5^\circ$  which represents the angle in the vicinity of  $\theta_{res}$ . Furthermore, the dots with lower frequency are near the curve of  $\theta_g$  and shift toward  $\theta_{res}$  with increase of frequency. That indicates strongly that the generation angle of the present chorus

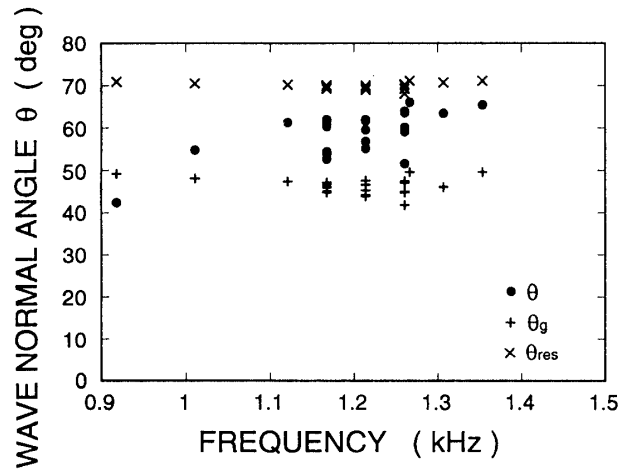


Fig. 7. The theoretical generation angle  $\theta_0$  obtained from three-dimensional inverse ray tracing computations. The corresponding Gendrin angle  $\theta_g$  and the oblique resonance angle  $\theta_{res}$  at the generation point are also plotted.

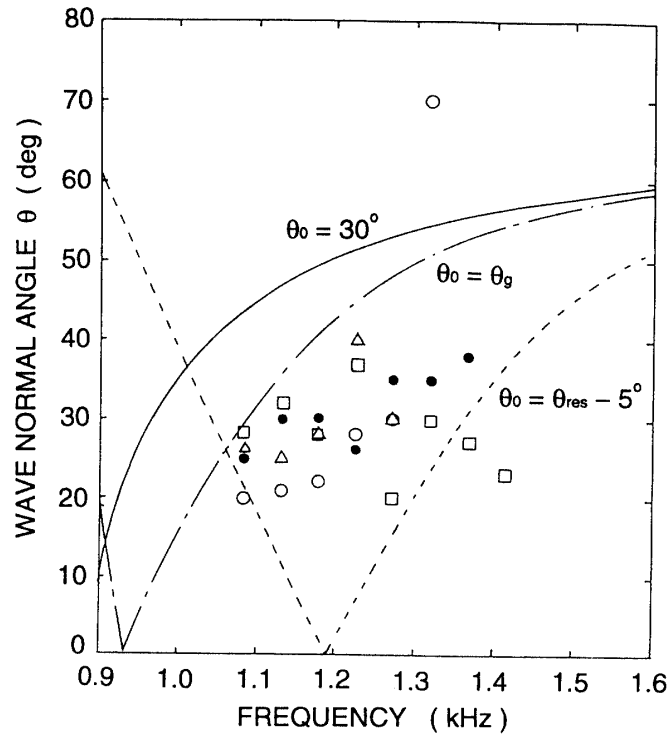


Fig. 8. The frequency dependence of the wave normal angle  $\theta$  observed onboard the satellite for the chorus elements. The different symbol refers to the different element. Supposing the analyzed chorus emissions occur with a fixed generation angle  $\theta_0$  in the generation region according to the proposed generation model, the expected  $\theta$  values detected onboard the satellite are also indicated. Three different  $\theta_0$ s are chosen.

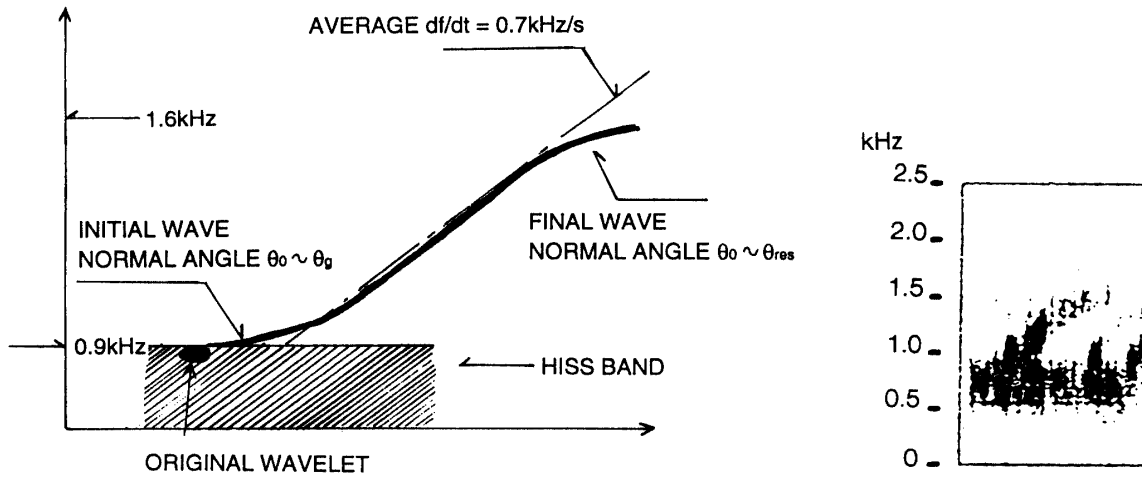


Fig. 9. Reconstructed and observed spectra.

element is near the Gendrin angle at the beginning and near the oblique resonance angle at the end. When we reconstruct a dynamic spectrum taking into account the above characteristics, the average value of  $df/dt$  is found to be about 0.7 kHz/s. Moreover, the tendency for small  $df/dt$  at the beginning of the chorus, which corre-

sponds to a gradual approach to the upper edge of the hiss band, is found to be well-reconstructed. The theoretically reconstructed chorus element also has a small  $df/dt$  around the uppermost frequencies. It is not so clear from the observed sonagrams, but a few chorus elements with the dynamic spectrum mentioned are found. Figure 9 shows the reconstructed and the observed dynamic spectra. Therefore, it is concluded that a possible generation model for hiss-triggered chorus is proposed from the standpoint of reconstruction of the dynamic spectra.

#### 4. Concluding Remarks

A possible generation mechanism of hiss-triggered chorus emission is presented based on experimental results and ray tracing computations from the standpoint of the temporal changes of frequency and the wave normal angle. It has two steps: phase bunching of resonant electrons by a causative wavelet and continuous radiation through cyclotron instability at different latitudes as the electrons travel away from the equator. This concept is based on the generation process of riser emissions in Helliwell's theory (HELLIWELL, 1967). The temporal variations of the dynamic spectra and the wave normal angle at the satellite location are theoretically reconstructed and investigated. Compared with the observed characteristics such as  $df/dt$  and the frequency dependence of wave normal angle for a chorus element, it is found that the chorus propagates in non-ducted mode. Furthermore, there is a tendency for the generation angle to be around the Gendrin angle at the beginning of the chorus; it becomes larger with increase of frequency, and finishes around the oblique resonance angle. This indicates the existence of the oblique instability, which means the off-magnetic field line instability. GOLDSTEIN and TSURUTANI (1984) suggested this tendency from the direction of chorus in the normalized frequency range of 0.3–0.5 which was observed in the generation region. The range of the normalized frequency of the chorus in the present paper is also 0.3–0.5. Therefore, the existence of the oblique instability is suggested not only for the spontaneous chorus but also the triggered chorus. The Gendrin angle is a specific angle in which the direction of energy propagation is parallel to the Earth's magnetic field lines except at the wave normal angle  $\theta = 0^\circ$  in the range of the normalized frequency less than 0.5. Therefore, the same effects in the case of the generation angle  $\theta_0 = 0^\circ$  are expected.

Taking account of the oblique instability, for example generation angle  $\theta_0 = \theta_g$  at the beginning of the chorus emission, the longitudinal energy required for the electrons in the cyclotron resonance with a wavelet at the upper edge of hiss band (0.9 kHz) is found to be about 3 keV. The relationship between the phase bunching time and the magnetic intensity for  $\theta_0 = \theta_g$  and  $\alpha_{eq} = 45^\circ$  is found to be almost the same in the cases of  $\theta_0 = 0^\circ$  and  $\alpha_{eq} = 45^\circ$ . Then, similar results are expected even when the generation angle  $\theta_0$  is varied with frequency or emission latitude. In order to investigate these points, computation of the growth rate may be required. This problem is closely related to chorus excitation from the causative wavelet in the hiss band mentioned in Section 3.1. Computer experiments are also feasible to explain the triggering process (OMURA *et al.*, 1991). But computer simulations mostly deal

with simple cases such as  $\theta_0 = 0^\circ$  because of the limited computer memory. In the present case, the assumption of the generation angle  $\theta_0 = 0^\circ$  itself seems not to be appropriate. However, OMURA and MATSUMOTO (1993) proposed long-time-scale (LTS) hybrid code simulation. It was found to be powerful in reproducing computation of triggering phenomena, both rising and falling tones.

We also have to refer to the importance of complementarity between the VLF active experiments at Siple station and the natural observations. Parallel propagating VLF waves with amplitude on the order of  $1\text{ m}\gamma$  can interact with cyclotron resonant electrons. Furthermore, VOMVORIDIS *et al.* (1982) reported the occurrence of triggered emissions from a VLF transmitter controlled by the relationship  $T \times P^{1/4}$ , where  $T$  and  $P$  correspond to the duration and the power of the injected pulse, respectively. For the present natural experiments, the hyperbolic threshold for triggering a chorus emission is obtained empirically as shown in Fig. 2, which is consistent with the criterion of the artificial experiments.

Natural observations, active injection experiments, and computer simulations should be compared. In the present paper, an approach based on the natural observations is performed. Investigation of the micro-process to explain how a causative wavelet triggers a chorus emission is a problem for the future.

### References

- BESPALOV, P. A. and TRAKHTENGERTS, V. Y. (1974): Nonstationary particles distribution in the magnetosphere and generation of periodic emissions in the VLF and SPP range. *Geomagn. Aeronom.*, **14**, 266–271.
- BURTIS, W. J. and HELLIWELL, R. A. (1976): Magnetospheric chorus: Occurrence patterns and normalized frequency. *Planet. Space Sci.*, **24**, 1007–1024.
- BURTON, R. K. and HOLZER, R. E. (1974): The origin and propagation of chorus in the outer magnetosphere. *J. Geophys. Res.*, **79**, 1014–1023.
- CORNILLEAU-WEHRLIN, N., GENDRIN, R., LEFEUVRE, F., PARROT, M., GRARD, R. *et al.* (1978): VLF waves observed onboard GEOS-1. *Space Sci. Rev.*, **22**, 371–382.
- CURTIS, S. A. (1978): A theory for chorus generation by energetic electrons during substorms. *J. Geophys. Res.*, **83**, 3841–3848.
- GOLDSTEIN, B. E. and TSURUTANI, B. T. (1984): Wave normal direction of chorus near equatorial source region. *J. Geophys. Res.*, **89**, 2789–2805.
- HATTORI, K., HAYAKAWA, M., LAGOUTTE, D., PARROT, M. and LEFEUVRE, F. (1991a): An experimental study of the role of hiss in generation of chorus in the outer magnetosphere, as based on detailed spectral analyses and direction finding measurements onboard GEOS 1. *Proc. NIPR Symp. Upper Atmos. Phys.*, **4**, 20–41.
- HATTORI, K., HAYAKAWA, M., LAGOUTTE, D., PARROT, M. and LEFEUVRE, F. (1991b): Further evidence of triggering chorus emissions from wavelets in the hiss band. *Planet. Space Sci.*, **39**, 1465–1472.
- HAYAKAWA, M., YAMANAKA, Y., PARROT, M. and LEFEUVRE, F. (1984): The wave normals of magnetospheric chorus emissions observed onboard GEOS-2. *J. Geophys. Res.*, **89**, 2811–2821.
- HAYAKAWA, M., HATTORI, K., SHIMAKURA, S., PARROT, M. and LEFEUVRE, F. (1990): Direction finding of chorus emissions in the outer magnetosphere and their generation and propagation. *Planet. Space Sci.*, **38**, 135–141.
- HELLIWELL, R. A. (1965): *Whistlers and Related Ionospheric Phenomena*. Stanford, Stanford Univ. Press.

- HELLIWELL, R. A. (1967): A theory of discrete VLF emissions from the magnetosphere. *J. Geophys. Res.*, **72**, 4773–4790.
- HELLIWELL, R. A., CARPENTER, D. L., INAN, U. S. and KATSUFRAKIS, J. P. (1986): Generation of band-limited VLF noise using the Siple transmitter: A model for magnetospheric hiss. *J. Geophys. Res.*, **91**, 4381–4392.
- KOONS, H. C. (1981): The role of hiss in magnetospheric chorus emissions. *J. Geophys. Res.*, **86**, 6745–6754.
- LUETTE, J. C., PARK, C. G. and HELLIWELL, R. A. (1977): Longitudinal variations of very low frequency chorus activity in the magnetosphere: Evidence of excitation by electrical power transmission lines. *Geophys. Res. Lett.*, **4**, 275–278.
- LUETTE, J. P., PARK, C. G. and HELLIWELL, R. A. (1979): The control of the magnetosphere by power line radiation. *J. Geophys. Res.*, **84**, 2657–2660.
- MATSUMOTO, H. and OMURA, Y. (1981): Cluster and channel effect phase bunching by whistler waves in the nonuniform geomagnetic field. *J. Geophys. Res.*, **86**, 779–791.
- MEANS, J. D. (1972): Use of the three dimensional covariance matrix in analyzing the polarization properties of plane waves. *J. Geophys. Res.*, **77**, 5551–5559.
- NUNN, D. (1974): A theoretical investigation of banded chorus. *J. Plasma Phys.*, **11**, 189–212.
- OMURA, Y., NUNN, D., MATSUMOTO, H. and RYCROFT, M. J. (1991): A review of observation, theoretical and numerical studies of VLF triggered emissions. *J. Atmos. Terr. Phys.*, **53**, 351–368.
- OMURA, Y. and MATSUMOTO, H. (1993): Electromagnetic and electrostatic waves in magnetospheric and laboratory plasmas: Theory, simulations and experiments. Abstracts, 24th General Assembly the URSI, Kyoto, Japan, 25 August – 2 September. 644.
- SA, L. A. D. (1990): A wave-particle-wave interaction mechanism as a cause of VLF triggered emissions. *J. Geophys. Res.*, **95**, 12277–12286.
- SAZHIN, S. S. (1982): *Natural Radio Emissions in the Earth's Magnetosphere*. Moscow, Nauka.
- SAZHIN, S. S. and HAYAKAWA, M. (1992): Magnetospheric chorus emissions: A review. *Planet. Space Sci.*, **40**, 681–697.
- SCHULZ, M. (1972): Intrinsic bandwidth of cyclotron resonance in the geomagnetic field. *Phys. Fluids*, **15**, 2448–2449.
- STOREY, L. R. O. and LEFEUVRE, F. (1979): The analysis of 6-component measurements of a random electromagnetic wave field in magneto-plasma -I The direct problem. *Geophys. J. R. Astron. Soc.*, **50**, 255–269.
- VOMVORIDIS, J. L., CARPENTER, T. L., INAN, U. S. and KATSUFRAKIS, J. P. (1982): Theory and computer simulations of magnetospheric very low frequency emissions. *J. Geophys. Res.*, **87**, 1473–1489.

*(Received June 1, 1993; Revised manuscript received October 20, 1993)*